Low Temperature Physics/Fizika Nizkikh Temperatur, 2021, vol. 47, No. 4, pp. 355–364

# Coronene-uracil complexes embedded in argon matrices: FTIR spectroscopy and quantum-mechanical calculations

S. G. Stepanian, A. Yu. Ivanov, and V. A. Karachevtsev

*B. Verkin Institute for Low Temperature Physics and Engineering of the National Academy of Sciences of Ukraine*
*Kharkiv 61103, Ukraine*
E-mail: stepanian@ilt.kharkov.ua

L. Adamowicz

*Department of Chemistry and Biochemistry, University of Arizona*
*Tucson, Arizona 85721, USA*

*Interdisciplinary Center for Modern Technologies, Nicolaus Copernicus University*
*Toruń 87-100, Poland*

Received October 31, 2020, published online February 26, 2021

We employ low-temperature matrix-isolation FTIR spectroscopy and quantum chemical calculations to study the interaction between nucleobase uracil and coronene which models the graphene surface. To observe the dimer FTIR spectrum, we use a quartz microbalance that allows us to produce matrix samples with precisely determined concentrations of coronene and uracil (with the concentration ratio of 2.5:1:1000 for coronene:uracil:argon). The interaction between coronene and uracil results in spectral shifts of uracil spectral bands. These shifts do not exceed 10 $cm^{-1}$. The maximum shifts are observed for the C=O stretching and NH out-of-plane vibrations of uracil. The structures and interaction energies of stacked and H-bonded coronene-uracil complexes are calculated at the DFT/B3LYP(GD3BJ)/aug-cc-pVDZ and MP2/aug-cc-pVDZ levels of theory. In total, 19 stable stacked and two H-bonded coronene-uracil dimer structures are found in the calculations. The interaction energy obtained for the most stable stacked dimer is – 12.1 and – 14.3 kcal/mol at the DFT and MP2 levels, respectively. The interaction energies of the H-bonded dimers do not exceed – 3 kcal/mol. The IR spectra of the studied monomeric molecules and of all the dimers are calculated at the DFT/B3LYP(GD3BJ)/aug-cc-pVDZ level of theory. The spectral shifts of the most stable stacked coronene-uracil dimer obtained in the calculations are in good agreement with the experimental results.

Keywords: low-temperature matrix isolation, FTIR spectroscopy, coronene, uracil, stacking.

## 1. Introduction

Significant interest in the study of hybrid materials based on graphene nanoparticles and graphene oxide also draws attention to polycyclic aromatic hydrocarbons (PAHs), as some of these systems, such as, for example, coronene ($C_{24}H_{12}$, Fig. 1), can be considered as simple models of the graphene surface [1–3]. It should also be noted that PAHs are also now a popular subject of astrophysical research due to their presence in the interstellar space. For example, PAHs were recently discovered in the atmosphere of Titan, as well as in a satellite of Saturn, by the Cassini–Huygens space probe mission [4]. It has been hypothesized that PAHs may be important intermediates in the formation of primitive organic molecules in outer space and in facilitating the creation of life in the universe. All this has stimulated interest in spectroscopic studies of the interaction of PAHs

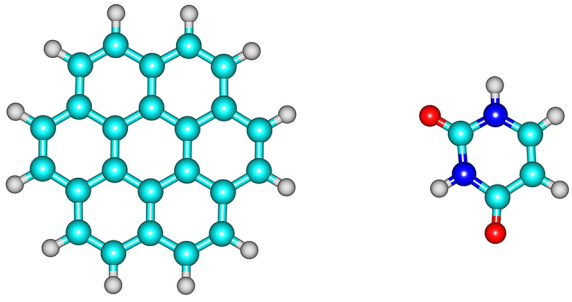


*Fig. 1.* Structure of the coronene and uracil molecules.

with molecular components of biomolecules, in particular, with nucleic acid bases. Importantly, unlike graphene, even relatively large PAHs, such as coronene ($C_{24}H_{12}$) or ovalene ($C_{32}H_{14}$), can be evaporated and moved intact to the gas phase. This makes it possible to use precision spectroscopic methods to study these systems. One of such methods is the low-temperature matrix-isolation FTIR spectroscopy.

IR spectra of coronene isolated in neon and argon matrices were studied previously [5, 6]. The first study of coronene isolated in a neon matrix [5] demonstrated that the vibrational frequencies of the matrix-isolated coronene molecule are close to the frequencies of coronene detected in the gas phase [7, 8] and that the band broadening is weak. In the subsequent study, Hudgins and Sandford analyzed the IR spectrum of coronene isolated in argon matrix [6] and showed that the IR spectrum of this system is quite simple due to its high symmetry ($D_{6h}$) [5, 6]. Only a subset of the coronene vibrations are active in IR spectra. The spectral bands of the matrix-isolated coronene are very sharp. Their half-width is about 1 $cm^{-1}$, which is significantly different from the spectra of coronene in the gas phase and in the condensed phase, where the characteristic half-widths of the bands are about 20 $cm^{-1}$. Another characteristic feature of the IR spectra of matrix-isolated coronene is the presence of a large number of combination bands in the 1950–1700 $cm^{-1}$ range of the spectrum [6].

The IR spectrum of the matrix-isolated uracil monomer is well studied [9–17]. It was shown that uracil is the only nucleobase that exists as a single (diketo) tautomer. This feature explains the choice of uracil as a component of the complexes with coronene studied in this work. The presence of only a single tautomer of uracil in the matrix significantly simplifies the analysis of the IR spectra of its intermolecular complexes. Despite the absence of multiple tautomers, in the region of the C=O stretching vibrations in the IR spectra of matrix-isolated uracil, instead of two bands ($C_2$=O str and $C_4$=O str), a significantly larger number of bands appear. Their presence is explained by multiple Fermi resonances between the fundamental C=O stretching vibrations and various combination vibrations [9–17].

The matrix isolation method is used not only to study monomeric molecules, but also molecular complexes [18–23]. An increase of the concentration of guest molecules in the matrix results in appearance of their homoassociates. However, the isolation of heteroassociates in matrices is much more difficult. Simultaneous increase of the concentrations of both components of a binary complex results in formation of both homo and heteroassociates in the matrices. The changes in the IR spectrum due to the formation of homoassociates are similar to the changes due to the formation of heteroassociates and this significantly complicates the analysis of the spectrum and, in most cases, makes it impossible to separate the spectra of the two types of associates. Earlier, it was shown that an effective way to obtain a higher concentration of the heteroassociates is to increase the concentration of only one components of the complex [21–23]. This approach is used in this work.

Samples with the ratio of coronene, uracil, and argon equal to 2.5:1:1000 are used in the present study. These samples contain uracil and coronene monomers, coronene dimers (due to higher concentration of coronene), and coronene-uracil dimers. This allows us to identify changes in the vibration frequencies of uracil appearing due to the formation of the complexes with coronene by comparing the vibration frequencies of the uracil monomer with the vibration frequencies of the uracil-coronene complexes. The preparation of the samples requires precise control of the concentrations of uracil and coronene in the matrix. For this we use a low-temperature quartz microbalance [24] to precisely control the coronene and uracil gas flows during the deposition of matrices.

The aim of this work is to identify the IR spectral manifestations of the interaction of coronene with uracil. Also, based on a comparison of the experimental IR spectra and the spectra calculated for various configurations of the uracil-coronene dimer, the configurations present in the matrices are identified.

## 2. Experimental methods and calculations

Low-temperature FTIR spectra of coronene and uracil (Sigma-Aldrich, USA) monomers, as well the coronene-uracil heterodimer, in argon matrices are recorded in the 3600–200 $cm^{-1}$ frequency range using the matrix isolation spectroscopy setup described in detail in the earlier works [24–27]. The apodised resolution of the frequency measurements is 0.3 $cm^{-1}$. During the matrix deposition, the molecular flows of the studied compounds are monitored using low-temperature quartz microbalances [24] and set to 10–50 ng/s $cm^2$ with the precision of ±1 %. The concentrations of coronene and uracil in the matrices (*M*/*S*, the matrix-to-sample ratio) are 1000:1. The evaporation of coronene for the monomer samples is done at the temperature of 460 K. The samples for studying the coronene-uracil heterodimers are prepared with *M*/*S* of 2.5:1:1000 (coronene:uracil:argon). The matrices are deposited onto a polished copper mirror at the temperature of 6 K. The purity of the matrix gas (Ar) used in the experiments is > 99.99 %. The evaporation of uracil and coronene from Knudsen cells for the heterodimers experiments is done at the temperatures of 445 K and 520 K, respectively. The Fityk software is used for deconvolution of the experimental bands into their constituents with the approximating functions being either Gaussians or Lorentzians [28].

The equilibrium structures and the corresponding harmonic IR spectra of the coronene and uracil monomers, as well their stacked and H-bonded complexes, are calculated using the DFT approach with the B3LYP density functional [29] and with the empirical dispersion correction, GD3BJ [30]. The standard aug-cc-pVDZ basis set [31] is used in the calculations. The interaction energies for the complexes are

calculated with accounting for the BSSE [32] and ZPVE corrections. The interaction energies of the most stable dimers are also calculated at the MP2/aug-cc-pVDZ level of theory to estimate the accuracy of the DFT/B3LYP(GD3BJ) calculations. All quantum-mechanical calculations are performed using the Gaussian 16 program package [33].

## 3. Results and discussion

### *3.1. Structures and relative stabilities of coronene-uracil dimers*

In searching for possible stacked structures of the coronene-uracil dimer, we first select 34 starting structures. In these structures, the uracil molecule is located in different positions relatively to the coronene molecule. Different distances between the uracil molecule and the center of the coronene molecule in the selected structures are chosen. The rotation of the uracil molecule is also considered in the selected starting structures. The direction of the displacement of the uracil molecule away from the center of the coronene is varied within 30° taking to account only directions which are unique within the $D_{6h}$ symmetry of the coronene molecule. The coronene-uracil dimer structure is fully optimized at the B3LYP(GD3BJ)/aug-cc-pVDZ level of theory with the optimizations starting with all the selected 34 initial structures. The optimizations are followed by the harmonic frequency calculations to verify that the equilibrium geometries found in the calculations are true minima on the dimer potential energy surface. No imaginary frequencies are found for any dimer geometry. The results of the frequency calculations are used to account for the ZPVE correction. The calculated IR spectra are subsequently used to analyze and assign the experimental spectra. Finally, the BSSE corrections are also calculated using the standard counterpoise procedure. In total, 19 unique stacked-dimer structures denoted as ST1–ST19 are identified among the 34 structures obtained in the calculations. The interaction energies for the 19 structures are shown in Table 1. The geometries of the 6 most stable coronene-uracil dimers are shown in Fig. 2. The interaction energy in the most stable dimer, ST1, is – 12.1 kcal/mol. It should be noted that the interaction energies of stacked dimers are close

Table 1. BSSE and ZPVE corrected interaction energies (*IE*, kcal/mol) calculated at the DFT/B3LYP(GD3BJ)/aug-cc-pVDZ and MP2/aug-cc-pVDZ levels of theory for stacked (ST) and H-bonded (HB) coronene-uracil dimers

| Dimer | $IE_{DFT}$ | $IE_{MP2}$ |
|---|---|---|
| ST1 | –12.1 | –14.3 |
| ST2 | –11.7 | –13.8 |
| ST3 | –11.5 | –13.5 |
| ST4 | –11.4 | |
| ST5 | –11.4 | |
| ST6 | –11.3 | |
| ST7 | –11.3 | |
| ST8 | –11.2 | |
| ST9 | –11.1 | |
| ST10 | –11.0 | |
| ST11 | –11.0 | |
| ST12 | –10.6 | |
| ST13 | –10.6 | |
| ST14 | –10.1 | |
| ST15 | –10.0 | |
| ST16 | –9.9 | |
| ST17 | –9.9 | |
| ST18 | –9.6 | |
| ST19 | –7.3 | |
| HB1 | –2.3 | |
| HB2 | –1.8 | |

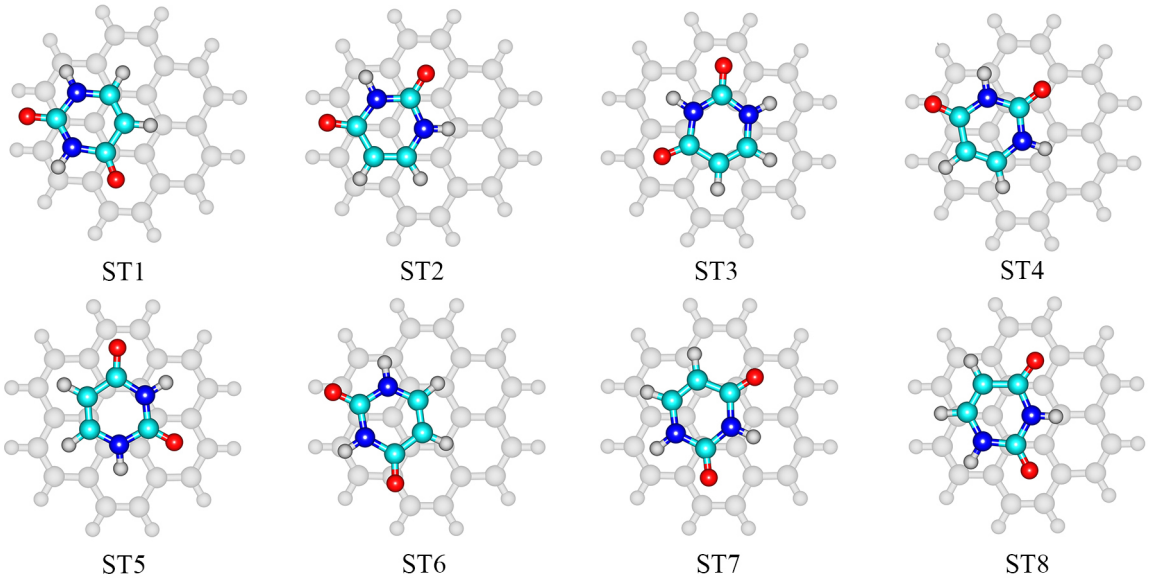


*Fig. 2.* Structures of the most stable coronene-uracil dimers calculated at the B3LYP(GD3BJ)/aug-cc-pVDZ level of theory.

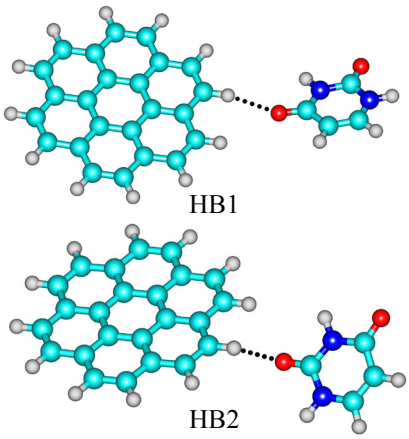


*Fig. 3.* Structures of the H-bonded coronene-uracil dimers calculated at the B3LYP(GD3BJ)/aug-cc-pVDZ level of theory.

and for the 10 most stable structures the differences in interaction energies are within 2 kcal/mol. This means that the presence of various dimer structures in the matrix can be expected.

The structures of the three most stable dimers are reoptimized at the MP2/aug-cc-pVDZ level of theory to check the reliability of the B3LYP(GD3BJ) geometry optimizations. The resulting ZPVE and BSSE corrected energies are shown in Table 1. As it is seen, the MP2 interaction energies are larger than the DFT energies by about 15–20 %. At the same time, the stability orders predicted by both methods are the same.

Calculations are also performed for hydrogen-bonded coronene-uracil dimers. These dimers are stabilized by a weak CH•••O hydrogen bond. Two dimer structures are found in the calculations (Fig. 3). They are denoted as HB1 and HB2. Their relative energies are given in Table 1. As expected, the intermolecular interaction in the H-bonded dimers is significantly weaker than in the stacked dimers. In the most stable H-bound dimer (HB1), the interaction energy is only - 2.3 kcal/mol, which is considerably less than for all stacked dimers. This suggests that formation of the H-bonded dimers in matrices is unlikely. In all stacked dimers, the contacts of the polar groups of uracil with the edge atoms of the coronene molecule are observed. To elucidate this effect further, calculations of charges on coronene atoms are performed with the Merz–Singh–Kollman scheme [34, 35]. The resulting charges and the distribution of the electrostatic potential in the most stable coronene-uracil dimer, ST1, are shown in Fig. 4. As can be seen, the terminal hydrogen and carbon atoms of the coronene molecule have relatively high charges. This indicates that the stacked dimers are stabilized not only by the dispersion interactions, but also by electrostatic interactions. Frontier orbitals of the ST1 dimer (Fig. 5) demonstrate the extent of overlapping of the π systems of coronene and uracil.

The calculations of the coronene-uracil dimer performed in this work demonstrate a complex shape of the potential energy surface of this system with multiple minima. In such

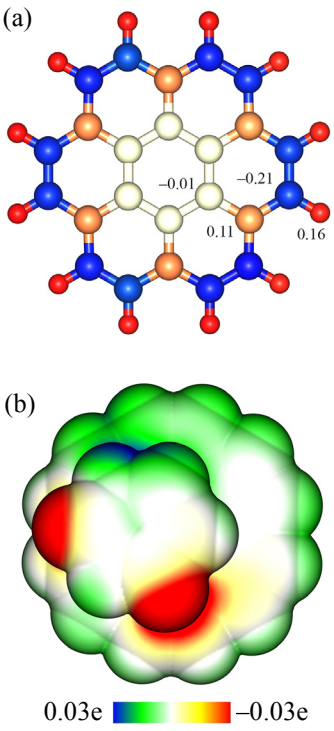


*Fig. 4.* Calculated atomic charges of the coronene molecule (a) and the electrostatic potential of the most stable coronene-uracil dimer, ST1 (b).

a case, important parameters to calculate are the energy barriers separating the local minima. If the values of these barriers are less than approximately 1 kcal/mol, interconversion between various structures is usually observed during the deposition of matrices [36]. The interconversion results in transitions of less stable structures to more stable ones. This process can significantly affect the composition of the matrix samples. To elucidate this effect, additional calculations of the values of the energy barriers for the coronene-uracil

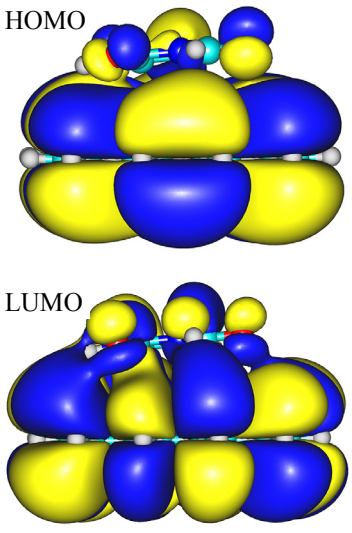


*Fig. 5.* Frontier molecular orbitals of the most stable coronene-uracil dimer ST1.

Table 2. Energy barriers ($E_{bar}$, kcal/mol) separating some minima on the potential energy surface of the coronene-uracil dimer calculated at the DFT/B3LYP(GD3BJ)/aug-cc-pVDZ levels of theory including accounting for the BSSE correction

| Transition | $E_{bar}$ |
|---|---|
| ST2 → ST1 | 0.47 |
| ST3 → ST2 | 0.19 |
| ST4 → ST2 | 0.29 |
| ST5 → ST3 | 0.17 |
| ST6 → ST1 | 0.16 |
| ST7 → ST3 | 0.22 |
| ST8 → ST7 | 0.43 |

system are performed. These calculations are carried out for pairs of dimers with similar structures, i.e., likely corresponding in adjacent local minima. The results of the calculations for the most stable dimers (ST1–ST8) are shown in Table 2. As it is seen, for all transitions from a less stable dimer to a more stable one, the barriers do not exceed 0.5 kcal/mol. This should lead to transitions of most of the higher-energy dimer structures predicted in the calculations to more stable configurations. Therefore, it can be assumed that only a small number of dimers exists in the matrix. An analysis of the experimental IR spectra performed next should show if the assumption is true.

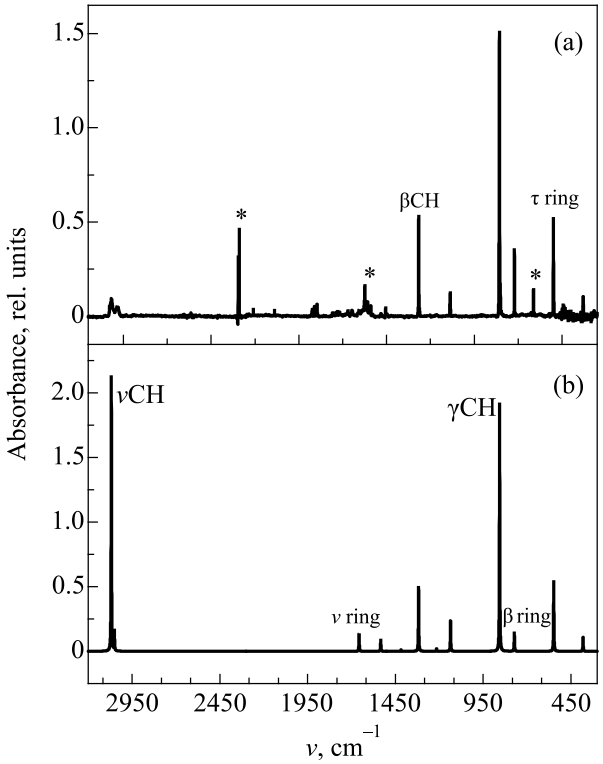


*Fig. 6.* Experimental FTIR spectrum of the matrix-isolated coronene (a) and graphical representation of calculated IR spectrum of coronene monomer (calculated at the B3LYP(GD3BJ)/aug-cc-pVDZ level of theory) (b).

### *3.2. FTIR spectra of the coronene and uracil monomers*

First, FTIR spectra of coronene and uracil monomers isolated in argon matrices are obtained. These spectra are used as a reference for the analysis of the dimer spectra. The obtained spectra, as well as a graphical representation of the IR spectra calculated with the B3LYP (GD3BJ) method are shown in Figs. 6 and 7. The frequencies and intensities of the coronene and uracil monomers are presented in Tables 3 and 4, respectively. A comparison of the experimental and calculated spectra shows very good agreement.

The comparison allows us to determine the optimal values of the scaling factors for the calculated spectral frequencies. These factors are determined to be 0.96 for the frequencies in the range over 2000 $cm^{-1}$ and 0.98 for frequencies in the range below 2000 $cm^{-1}$. After scaling of the calculated frequencies, the average difference between the observed and predicted vibrational frequencies is about 5 $cm^{-1}$. The only exception is the region of the C=O stretching vibrations of uracil (1800–1700 $cm^{-1}$). The reason for the larger discrepancies in this range is the splitting of the absorption bands of uracil due to the Fermi resonance between the C=O stretching vibrations and combinational vibrations or/and overtones.

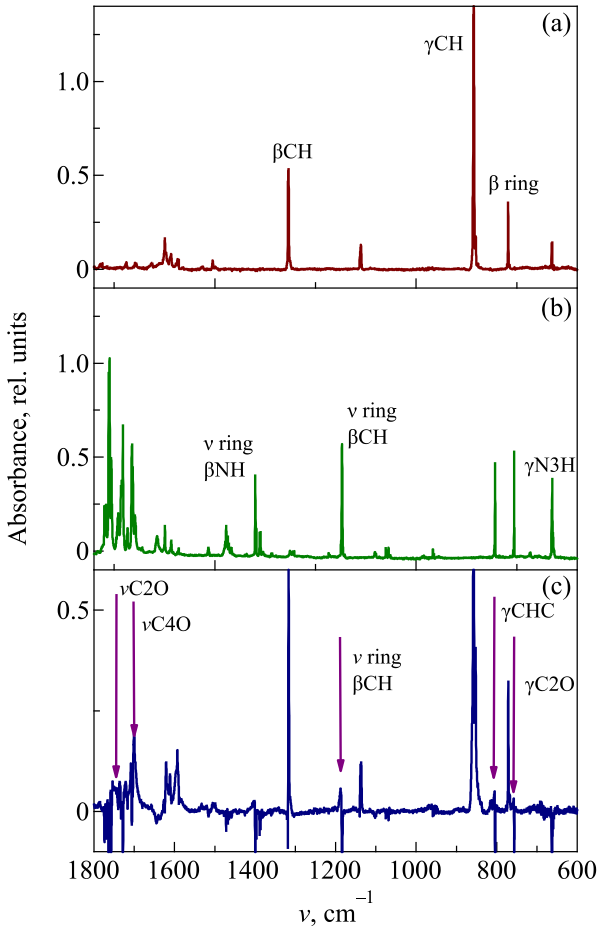


*Fig. 7.* Experimental FTIR spectrum of the matrix-isolated coronene (a), uracil (b), and coronen-uracil dimer (c).

Table 3. Experimental ($\nu_e$, cm$^{-1}$, $I_{rel}$, rel. units) (Ar matrix) and selected calculated at the B3LYP(GD3BJ)/aug-cc-pVDZ level of theory ($\nu_c$, cm$^{-1}$, $I_c$, km/mol) frequencies and intencities of the coronene monomer. The frequency scaling factors are 0.98 (< 2000 cm$^{-1}$) and 0.96 (> 2000 cm$^{-1}$). $I_{rel}$ is experimental relative integral intensities

| Ar matrix | | Calculated | | |
|---|---|---|---|---|
| $\nu_e$ | $I_{rel}$ | $\nu_c$ | $I_c$ | Assignment |
| 3077.1 | 0.21 | | | |
| 3072.3 | 0.37 | | | |
| 3067.2 | 0.67 | 3059 | 85.0 | CH str |
| 3065.6 | 0.35 | | | |
| 3056.8 | 0.12 | | | |
| 3051.9 | 0.13 | 3056 | 0.7 | CH str |
| 3044.3 | 0.17 | | | |
| 3039.7 | 0.12 | | | |
| 3035.0 | 0.28 | 3041 | 6.4 | CH str |
| 3028.8 | 0.24 | | | |
| 1924.0 | 0.15 | | | |
| 1911.2 | 0.22 | | | |
| 1896.5 | 0.25 | | | |
| 1808.2 | 0.05 | | | |
| 1799.8 | 0.06 | | | |
| 1783.6 | 0.27 | | | |
| 1720.5 | 0.26 | | | |
| 1697.2 | 0.26 | | | |
| 1657.0 | 0.28 | 1624 | 5.4 | C-C str |
| 1531.4 | 0.08 | | | |
| 1505.1 | 0.14 | 1503 | 3.8 | C-C str |
| 1498.2 | 0.05 | | | |
| 1318.2 | 0.36 | | | |
| 1317.0 | 1.25 | 1312 | 19.9 | ring str, CH bend |
| 1313.2 | 0.19 | | | |
| 1140.0 | 0.06 | | | |
| 1138.2 | 0.24 | | | |
| 1136.8 | 0.25 | 1131 | 9.3 | CH bend |
| 858.7 | 0.97 | | | |
| 857.8 | 1.34 | 852 | 151.2 | CH out-of-plane |
| 857.1 | 0.99 | | | |
| 856.4 | 0.87 | | | |
| 855.8 | 1.0 | | | |
| 852.0 | 0.38 | | | |
| 774.0 | 0.02 | | | |
| 771.6 | 0.39 | 768 | 6.0 | ring bend |
| 771.0 | 0.14 | | | |
| 767.9 | 0.03 | | | |
| 550.3 | 0.26 | | | |
| 549.6 | 0.59 | 545 | 43.2 | ring bend |
| 548.7 | 0.41 | | | |
| 547.7 | 0.1 | | | |
| 546.9 | 0.16 | | | |
| 380.1 | 0.06 | 379 | 4.3 | ring out-of-plane |
| 378.8 | 0.08 | | | |

Table 4. Experimental FTIR spectrum of uracil monomer (frequencies: $\nu_e$, cm$^{-1}$, integral relative intensities: $I_{rel}$, rel. units) and experimental differential spectrum of the coronene-uracil dimer (the spectrum of uracil monomers is subtracted from the spectrum of the complex). Harmonic vibrational spectra of uracil monomer and uracil moiety in the coronene-uracil dimer are calculated at the B3LYP(GD3BJ)/aug-cc-pVDZ level of theory ($\nu_c$, cm$^{-1}$, $I_c$, km/mol). Scaling factors are 0.98 (< 2000 cm$^{-1}$) and 0.96 (> 2000 cm$^{-1}$)

| Observed (Ar matrix) | | | | Calculated | | | | |
|---|---|---|---|---|---|---|---|---|
| Uracil monomer | | Differential spectrum | | Uracil monomer | | Dimer ST1 | | Assignment |
| $\nu_e$ | $I_{rel}$ | $\nu_e$ | $I_{rel}$ | $\nu_c$ | $I_c$ | $\nu_c$ | $I_c$ | |
| 1 | 2 | 3 | 4 | 5 | 6 | 7 | 8 | 9 |
| 1780.3 | 0.16 | | | | | | | |
| 1773.7 | 0.97 | 1771.6 | 0.05 | | | | | |
| 1769.9 | 0.59 | | | | | | | |
| 1763.4 | 1.64 | 1765.8 | 0.02 | | | | | |
| 1761.3 | 2.23 | | | 1756 | 625.6 | | | C2O str |
| 1756.9 | 1.52 | 1758.7 | 0.2 | | | | | |
| 1755.3 | 0.32 | 1754.9 | 0.3 | | | 1745 | 374.6 | C2O str |
| 1740.3 | 1.53 | 1737.1 | 0.16 | | | | | |
| 1732.5 | 1.36 | | | | | | | |
| 1730.3 | 0.74 | | | | | | | |
| 1728.1 | 0.99 | | | 1725 | 764.1 | | | C4O str |
| 1719.0 | 0.21 | | | | | | | |
| 1717.9 | 0.1 | | | | | 1714 | 433.5 | C4O str |

Continuation of the Table 4

| Observed (Ar matrix) | | | | Calculated | | | | |
|---|---|---|---|---|---|---|---|---|
| Uracil monomer | | Differential spectrum | | Uracil monomer | | Dimer ST1 | | Assignment |
| $\nu_e$ | $I_{rel}$ | $\nu_e$ | $I_{rel}$ | $\nu_c$ | $I_c$ | $\nu_c$ | $I_c$ | |
| 1 | 2 | 3 | 4 | 5 | 6 | 7 | 8 | 9 |
| 1716.6 | 0.08 | | | | | | | |
| | | 1708.9 | 0.03 | | | | | |
| 1705.8 | 1.78 | | | | | | | |
| 1703.6 | 1.33 | 1700.4 | 0.73 | | | | | |
| 1697.7 | 1.34 | | | | | | | |
| 1685.0 | 0.05 | | | | | | | |
| 1679.9 | 0.05 | | | | | | | |
| 1643.5 | 0.69 | | | 1642 | 48.8 | 1641 | 24.3 | ring str |
| 1516.1 | 0.15 | | | | | | | |
| 1473.9 | 0.1 | | | | | | | |
| 1471.6 | 0.54 | | | | | | | |
| 1467.6 | 0.04 | 1469.2 | 0.01 | 1468 | 89.2 | 1470 | 41.5 | NH bend |
| 1464.8 | 0.11 | | | | | | | |
| 1458.3 | 0.12 | | | | | | | |
| 1399.5 | 0.48 | 1403.0 | 0.08 | 1384 | 46.1 | 1388 | 36.7 | CH bend, NH bend |
| 1398.4 | 0.26 | | | | | | | |
| 1396.8 | 0.07 | | | | | | | |
| 1388.5 | 0.17 | 1387.6 | 0.01 | 1375 | 61.9 | 1378 | 23.0 | NH bend, ring str |
| 1386.2 | 0.1 | | | | | | | |
| 1380.2 | 0.14 | | | | | | | |
| 1359.2 | 0.03 | | | 1352 | 21.3 | 1353 | 7.4 | ring str, NH bend |
| 1357.4 | 0.02 | | | | | | | |
| 1306.1 | 0.03 | | | | | | | |
| 1302.8 | 0.02 | | | | | | | |
| 1217.4 | 0.04 | | | 1203 | 0.4 | 1205 | 0.3 | CH bend, ring str |
| 1186.5 | 0.13 | 1187.6 | 0.13 | 1173 | 106.7 | 1177 | 51.8 | NH def, CH def |
| 1184.1 | 1.42 | 1185.9 | 0.03 | | | | | |
| 1102.2 | 0.11 | | | | | | | |
| 1075.2 | 0.06 | | | | | | | |
| 1068.3 | 0.07 | | | 1065 | 6.3 | 1066 | 1.9 | CH bend |
| 958.2 | 0.11 | | | 969 | 7.3 | 974 | 7.7 | ring def |
| | | | | 948 | 0.3 | 951 | 5.1 | CH oop |
| | | | | 946 | 8.6 | 947 | 1.2 | NH def, CH def |
| 805.5 | 0.15 | 805.0 | 0.1 | 804 | 60.6 | 798 | 73.0 | CH oop |
| 804.0 | 0.57 | 807.0 | 0.05 | | | | | |
| 757.7 | 0.16 | 757.5 | 0.07 | 757 | 3.0 | 751 | 0.2 | ring def, ring str |
| 756.5 | 0.32 | | | 748 | 37.5 | 742 | 60.2 | ring oop |
| 717.1 | 0.05 | | | 712 | 17.7 | 707 | 20.0 | CH oop |
| 662.0 | 0.75 | | | 682 | 63.6 | 657 | 82.4 | N3H oop |
| 551.1 | 0.17 | | | 569 | 43.0 | 552 | 89.1 | N1H oop |
| | | | | 546 | 5.4 | 547 | 40.5 | ring def |
| 536.3 | 0.09 | | | 529 | 5.4 | 530 | 4.1 | ring def |
| 516.2 | 0.23 | | | 509 | 21.4 | 508 | 10.3 | ring def |
| 514.0 | 0.09 | | | | | | | |
| | | | | 377 | 21.4 | 377 | 10.6 | CO bend |
| | | | | 166 | 0.0 | 161 | 2.2 | ring oop |
| | | | | 149 | 2.1 | 142 | 12.9 | ring oop |

### 3.3. FTIR spectra of the coronene-uracil complexes

To identify the experimental IR spectral bands of the coronene-uracil dimer, a matrix IR spectrum of the uracil monomer and the spectrum of the coronene-uracil dimer are measured. As noted earlier, the dimer spectrum is obtained for samples with $M/S = 2.5{:}1{:}1000$ (coronene:uracil:argon). In addition to the coronene-uracil dimer, these samples contain the uracil monomer, as well as the coronene monomer and its dimers. Now, the main task is to identify the spectral bands of uracil forming the dimer with coronene. For this, a differential IR spectrum is calculated by subtracting the spectrum of the of the uracil monomer from the spectrum obtained for the coronene-uracil sample. The resulting differential spectrum (range 1800–400 $cm^{-1}$) is shown in Fig. 7. The figure also shows the spectrum of the uracil monomer. As can be seen in the IR spectrum of the coronene-uracil system, a significant decrease in the intensity of some bands of the uracil monomer appears. This effect is due to the formation of the coronene-uracil dimer. Also, new bands appear in the IR spectrum (in Fig. 7(c) they are marked). The vibration frequencies corresponding to the new bands differ by a few inverse centimeters from the corresponding vibrational frequencies of the uracil monomer. This allows us to conclude that the new bands can be attributed to the vibrations of uracil forming the dimer with coronene.

The experimental and calculated vibrational frequencies and intensities of the uracil monomer and the coronene-uracil dimer are shown in Table 4. As can be seen, the calculated shifts of the uracil vibration bands due to the formation of the dimer with coronene are in good agreement with the experimental data. In total, six new bands corresponding to the vibrations of uracil forming the dimer with coronene are identified. Both the experiment and the calculations are in agreement in showing that the maximal spectral shifts of the uracil bands due to dimerization are occurring for the C=O stretching and NH out-of-plane vibrations (Fig. 8). For these vibrations the experimental shift is about 10 $cm^{-1}$. It should

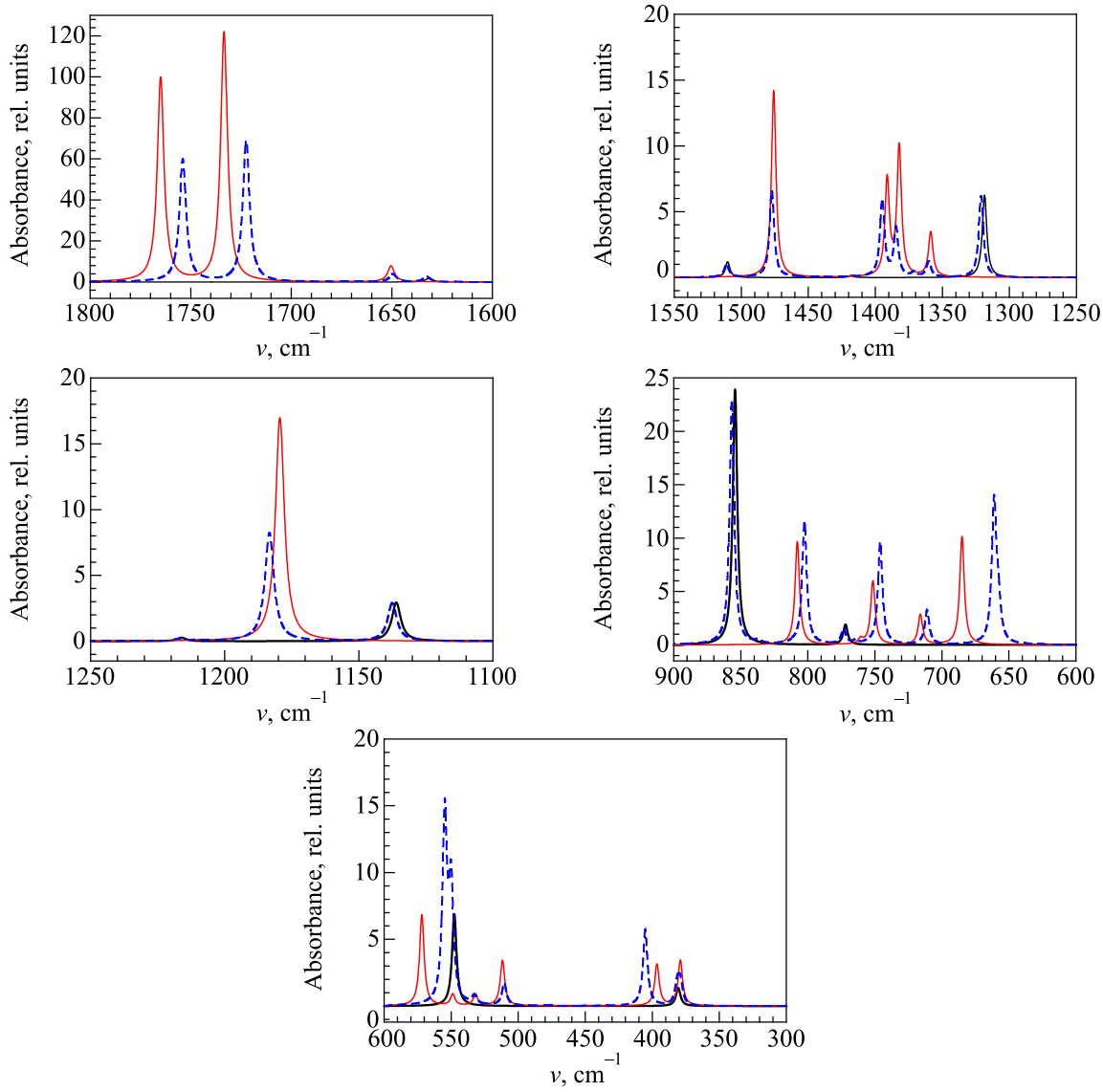


*Fig. 8.* (Color online) Graphical representation of the IR spectra of coronene (solid black line), uracil (solid red line), and coronene-uracil dimer (dashed blue line) calculated at the B3LYP(GD3BJ)/aug-cc-pVDZ level of theory.

also be noted that the experimental spectral manifestations of the formation of coronene-uracil dimer are in good agreement with the calculations performed for the most stable dimer, ST1. The strong prevalence of ST1 in the matrix is consistent with the results of the calculations of the energy barriers separating various configurations of the coronene-uracil dimer in the potential energy surface which showed the possibility of interconversion of most dimers to the most stable ST1 configuration.

The information presented in this work on the IR spectra, the interaction energy, and the structure of the coronene-uracil dimer can be, for example, useful in designing and fabrication of such a new class of fluorescent nanomaterials as graphene quantum dots which have attracted considerable attention due to their outstanding properties and potential applications in nanomedicine as nanosized scaffolds for drug delivery and bioimaging [37]. The information can also be useful in fabrication of biosensors based on the graphene field-force transistor with adsorbed DNA. Such sensors can be employed in optoelectronics and energy-related fields.

## 4. Conclusions

In this work, coronene-uracil dimers are isolated in low-temperature argon matrices and studied with the IR spectroscopy and with quantum-chemical calculations. The samples with matrix ratio 2.5:1:1000 (coronen:uracil:argon) are prepared with the coronene and uracil concentrations precisely controlled using a low-temperature quartz microbalance. The coronene-uracil dimer can be considered as the simplest model of a biological molecule (nucleobase) adsorbed on the graphene surface. The quantum-chemical calculations are employed in this work to study the structure and the interaction between uracil and coronene. This interaction results in spectral shifts of uracil bands. The shifts do exceed 10 $cm^{-1}$ with the maximal shifts observed for the uracil C=O stretching and NH out-of-plane vibrations. The structures and the interaction energies of stacked and H-bonded coronene-uracil complexes are calculated at the DFT/B3LYP(GD3BJ)/aug-cc-pVDZ and MP2/aug-cc-pVDZ levels of theory. In total, 19 stable stacked and 2 H-bonded coronene-uracil dimer structures are identified. The interaction energies obtained for the most stable stacked dimer are –12.1 and –14.3 kcal/mol at the DFT and MP2 levels, respectively. The interaction energies of the H-bonded dimers do not exceed –2.3 kcal/mol. Energy barriers separating some of the lowest energy minima on the potential energy surface of the coronene-uracil dimer are calculated. The energy-barrier calculations are carried out for pairs of dimers with similar structures located in adjacent local minima of the potential energy surface. The calculated barriers do not exceed 0.5 kcal/mol. Such low barriers likely lead to transitions of most of the higher-energy dimer structures predicted in the calculations to more stable configurations. Therefore, it can be assumed that only a small number of dimers exist in the matrix. IR spectra of the coronene and uracil molecules and their dimers are calculated at the DFT/B3LYP(GD3BJ)/aug-cc-pVDZ level of theory. The results are used to calculate the shifts of the uracil spectral lines. The shifts, which are due to the interaction between coronene and uracil molecules, are in good agreement with the experimental results. The electrostatic potential of the coronene-uracil dimers demonstrates that the terminal hydrogen and carbon atoms of the coronene molecule have relatively high charges. This shows that the stacked dimers are stabilized not only by the dispersion interactions but also by Coulombic interactions.

This work was supported by the National Academy of Sciences of Ukraine (under Grant No. 0120U100157). An allocation of computer time from the Computational Center at Institute for Low Temperature Physics and Engineering and from UA Research High Performance Computing (HPC) and High Throughput Computing (HTC) at the University of Arizona is gratefully acknowledged.

1. Z. Zhang, H. Huang, X. Yang, and L. Zang, *J. Phys. Chem. Lett.* **2**, 2897 (2011).
2. B. Saha and P. K. Bhattacharyya, *ACS Omega* **3**, 16753 (2018).
3. J. P. A. de Mendonça, A. H. de Lima, G. M. A. Junqueira, W. G. Quirino, C. Legnani, I. O. Maciel, and F. Sato, *Mater. Res. Express* **3**, 055020 (2016).
4. M. López-Puertas, B. M. Dinelli, A. Adriani, B. Funke, M. García-Comas, M. L. Moriconi, E. D'Aversa, C. Boersma, and L. J. Allamandola, *Astrophys. J.* **770**, 132 (2013).
5. C. Joblin, L. d'Hendecourt, A. Léger, and D. Défourneau, *Astron. Astrophys.* **281**, 923 (1994).
6. D. M. Hudgins and S. A. Sandford, *J. Phys. Chem. A* **102**, 344 (1998).
7. R. J. H. Clark and R. E. Hester, *Spectroscopy of Matrix Isolated Species*, Wiley, New-York (1989).
8. C. Joblin, L. d'Hendecourt, A. Léger, and D. Défourneau, *Astr. Astrophys*. **281**, 923 (1994).
9. E. D. Radchenko, A. M. Plokhotnichenko, G. G. Sheina, and Yu. P. Blagoi, *Biofizika* **28**, 923 (1983) (in Russian).
10. Yu. P. Blagoi, E. D. Radchenko, S. G. Stepanian, and G. G. Sheina, *J. Mol. Struct.* **219**, 311 (1990).
11. M. Szczesniak, M. J. Nowak, H. Rostkowska, W. B. Person, and D. Shugar, *J. Am. Chem. Soc.* **105**, 5969 (1983).
12. M. Szczesniak, M. J. Nowak, K. Szczepaniak, S. Chin, L. Scott, and W. B. Person, *Spectrochim. Acta, Part A* **41**, 223 (1985).
13. A. J. Barnes, M. A. Stuckey, and L. Le Gall, *Spectrochim. Acta, Part A* **40**, 419 (1984).
14. M. Maltese, S. Passerini, S. Nunziante-Cesaro, S. Dobos, and L. Harsanyi, *J. Mol. Struct.* **116**, 49 (1984).
15. M. J. Nowak, *J. Mol. Struct.* **193**, 35 (1989).
16. M. Graindourze, J. Smets, Th. Zeegers-Huyskens, and G. Maes, *J. Mol. Struct.* **222**, 345 (1990).
17. A. Les, L. Adamowicz, M. J. Nowak, and L. Lapinski, *Spectrochim. Acta, Part A* **48**, 1385 (1991).

18. W. MacCarthy, J. Smets, L. Adamowicz, A. M. Plokhotnichenko, E. D. Radchenko, G. G. Sheina, and S. G. Stepanian, *Molec. Phys*. **91**, 513 (1997).
19. A. M. Plokhotnichenko, E. D. Radchenko, S. G. Stepanian, and L. Adamowicz, *J. Phys. Chem. A* **103**, 1052 (1999).
20. A. M. Plokhotnichenko, E. D. Radchenko, Yu. P. Blagoi, and V. A. Karachevtsev, *Fiz. Nizk. Temp.* **27**, 901 (2001) [*Low Temp. Phys*. **27**, 666 (2001)].
21. W. MacCarthy, A. M. Plokhotnichenko, E. D. Radchenko, J. Smets, D. M. A. Smith, S. G. Stepanian, and L. Adamowicz, *J. Phys. Chem. A* **101**, 7208 (1997).
22. A. M. Plokhotnichenko, S. G. Stepanian, L. Adamowicz, and V. A. Karachevtsev, *Fiz. Nizk. Temp.* **32**, 201 (2006). [*Low Temp. Phys.* **32**, 148 (2006)].
23. A. M. Plokhotnichenko, S. G. Stepanian, and L. Adamowicz, *Chem. Phys. Lett.* **608**, 84 (2014).
24. A. Yu. Ivanov and A. M. Plokhotnichenko, *Instrum. Exp. Tech*. **52**, 308 (2009).
25. A. Yu. Ivanov, A. M. Plokhotnichenko, E. D. Radchenko, G. G. Sheina, and Yu. P. Blagoi, *J. Mol. Struct.* **372**, 91 (1995).
26. A. Yu. Ivanov, S. A. Krasnokutski, G. Sheina, and Yu. P. Blagoi, *Spectrochim. Acta A* **59**, 1959 (2003).
27. A. Yu. Ivanov and V. A. Karachevtsev, *Fiz. Nizk. Temp*. **33**, 772 (2007) [*Low Temp. Phys.* **33**, 590 (2007)].
28. M. Wojdyr, *J. Appl. Cryst*. **43**, 1126 (2010).
29. A. D. Becke, *Phys. Rev. A* **38**, 3098 (1988).
30. S. Grimme, S. Ehrlich, and L. Goerigk, *J. Comp. Chem.* **32**, 1456 (2011).
31. T. H. Dunning, Jr., *J. Chem. Phys.* **90**, 1007 (1989).
32. S. F. Boys and F. Bernardi, *Mol. Phys*. **19**, 553 (1970).
33. *Gaussian 16, Revision B.01*, M. J. Frisch, G. W. Trucks, H. B. Schlegel, G. E. Scuseria, M. A. Robb, J. R. Cheeseman, G. Scalmani, V. Barone, G. A. Petersson, H. Nakatsuji, X. Li, M. Caricato, A. V. Marenich, J. Bloino, B. G. Janesko, R. Gomperts, B. Mennucci, H. P. Hratchian, J. V. Ortiz, A. F. Izmaylov, J. L. Sonnenberg, D. Williams-Young, F. Ding, F. Lipparini, F. Egidi, J. Goings, B. Peng, A. Petrone, T. Henderson, D. Ranasinghe, V. G. Zakrzewski, J. Gao, N. Rega, G. Zheng, W. Liang, M. Hada, M. Ehara, K. Toyota, R. Fukuda, J. Hasegawa, M. Ishida, T. Nakajima, Y. Honda, O. Kitao, H. Nakai, T. Vreven, K. Throssell, J. A. Montgomery, Jr., J. E. Peralta, F. Ogliaro, M. J. Bearpark, J. J. Heyd, E. N. Brothers, K. N. Kudin, V. N. Staroverov, T. A. Keith, R. Kobayashi, J. Normand, K. Raghavachari, A. P. Rendell, J. C. Burant, S. S. Iyengar, J. Tomasi, M. Cossi, J. M. Millam, M. Klene, C. Adamo, R. Cammi, J. W. Ochterski, R. L. Martin, K. Morokuma, O. Farkas, J. B. Foresman, and D. J. Fox, Gaussian, Inc., Wallingford CT, 2016.
34. U. C. Singh and P. A. Kollman, *J. Comp. Chem.* **5**, 129 (1984).
35. B. H. Besler, K. M. Merz, Jr., and P. A. Kollman, *J. Comp. Chem.* **11**, 431 (1990).
36. S. G. Stepanian, A. Yu. Ivanov, and L. Adamowicz, *Chem. Phys*. **423**, 20 (2013).
37. W. Chen, G. Lv, W. Hu, D. Li, S. Chen, and Z. Dai, *Nanotechnol. Rev.* **7**, 157 (2018).

## Комплекси коронен-урацил в аргонових матрицях: ІЧ фур'є-спектроскопія та квантово-механічні розрахунки

S. G. Stepanian, A. Yu. Ivanov, V. A. Karachevtsev, L. Adamowicz

Застосовано матричну ІЧ фур'є-спектроскопію та квантово-хімічні розрахунки для вивчення взаємодій між нуклеїновою основою урацилом та короненом, який моделює поверхню графена. Використання кварцових мікроваг дозволило отримати матричні зразки з точними концентраціями коронену та урацилу (матричне співвідношення 2.5:1:1000, коронен:урацил:аргон). Встановлено, що взаємодія між короненом та урацилом призводить до спектральних зсувів смуг урацилу, які не перевищують 10 см$^{-1}$. Максимальні зсуви спостерігались для валентних коливань C=O груп та позаплощинних коливань NH груп урацилу. Структура та енергії взаємодії стекінг та H-зв'язаних комплексів коронен-урацил розраховано з використанням методів DFT/B3LYP(GD3BJ)/aug-cc-pVDZ та MP2/aug-cc-pVDZ. Всього знайдено 19 стабільних стекінг та два H-зв'язаних димерів коронен-урацил. Енергії взаємодії, які отримані для найбільш стабільного стекінг-димеру, становили –12,1 та –14,3 ккал/моль для методів DFT та MP2. Енергії взаємодії в H-зв'язаних димерах не перевищували –3 ккал/моль. ІЧ спектри досліджених мономерних молекул та всіх димерів розраховано з використанням методу DFT/B3LYP(GD3BJ)/aug-cc-pVDZ. Отримані спектральні зсуви, які є наслідком взаємодії коронену та урацилу, добре узгоджуються з експериментальними результатами у випадку найбільш стабільного димеру.

Ключові слова: низькотемпературна матрична ізоляція, ІЧ спектроскопія, коронен, урацил, стекінг.